



Macromolecular Nanotechnology

SANS study on self-assembled structures of glucose-responsive phenylboronate ester-containing diblock copolymer

Yunyan Zhang^a, Wenwen Zhao^a, Junjiao Yang^b, Boualem Hammouda^c, Jing Yang^{a,d,*}, Gang Cheng^{a,*}^a College of Life Science and Technology, Beijing University of Chemical Technology, Beijing 100029, China^b College of Science, Beijing University of Chemical Technology, Beijing 100029, China^c Center for Neutron Research, National Institute of Standards and Technology, Gaithersburg, MD 20899, USA^d State Key Laboratory of Chemical Resource, Beijing University of Chemical Technology, Beijing 100029, China

ARTICLE INFO

Article history:

Received 5 June 2016

Received in revised form 18 July 2016

Accepted 17 August 2016

Available online 20 August 2016

Keywords:

SANS

Glucose responsive

Vesicles

Phenylboronate ester

Phenylboronic acid

ABSTRACT

Block copolymers containing boronic acid-functionalized segments belong to an interesting class of materials that can be potentially used in developing self-regulated insulin delivery systems. Determination of the solution structure of these block copolymers is crucial to understanding their performance. Self-assembled structures of glucose-responsive diblock copolymer, poly(ethyleneglycol)-block-poly[(2-phenylboronate esters-1,3-dioxane-5-ethyl)methylacrylate] (PEG-b-PPBDEMA), in aqueous solution were studied using small-angle neutron scattering (SANS). SANS data suggested that PEG-b-PPBDEMA diblock copolymer with a PEG content of 24 wt.% formed vesicles that responded differently to 0.1% and 0.5 wt.% glucose under physiological conditions. Upon elevation of pH, a shape transition to cylinders was observed. The effect of molarity of the buffer on the stability of the vesicles and micelles was also studied.

© 2016 Elsevier Ltd. All rights reserved.

1. Introduction

Over the past decade, the biomedical applications of boronic acid-containing polymers have been extensively studied because of their ability to form esters with 1, 2- or 1, 3-diols [1,2]. Boronic acids are not soluble in water when the pH of the environment is less than their pK_a . Increased ionization upon elevation of pH or reaction with diols takes place, leading to improved solubility in water [3]. This shift in solubility upon complexation with diols allows for the construction of sugar responsive materials, i.e., nanogels, micelles, and vesicles [1,2]. Block copolymers with one of the blocks containing phenylboronic acids (PBAs) have been frequently tested as self-regulated insulin delivery systems for treating diabetes [1,2,4–6]. They undergo self-assembly in water to form nanostructures (micelles and vesicles) due to hydrophobicity of the boronic acid segment at $pH < pK_a$. These nanostructures swell or dissociate with addition of glucose. However, one of the shortcomings with PBA-containing block copolymers is that PBAs can only efficiently bind with diols near or above the pK_a of the PBAs, which is usually above the physiological pH, for example, poly(3-acrylamidophenylboronic acid) has a pK_a of about 9 [1,2]. Different approaches have been developed to achieve glucose responsiveness at physiological pH, including coordination of Lewis bases with the boron center, introduction of electron-withdrawing groups, and use of benzoxaboroles [2].

* Corresponding authors at: College of Life Science and Technology, Beijing University of Chemical Technology, Beijing 100029, China (J. Yang, G. Cheng).
E-mail addresses: yangj@mail.buct.edu.cn (J. Yang), chenggang@mail.buct.edu.cn (G. Cheng).

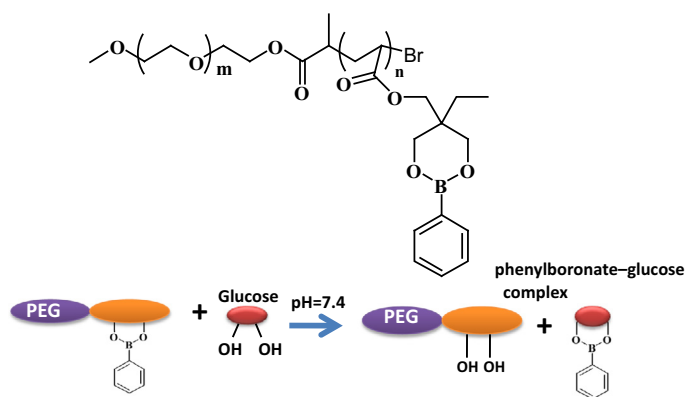


Fig. 1. Chemical structure of the diblock copolymer PEG-b-PPBDEMA and its reaction with glucose.

In general, boronic esters have a pK_a slightly lower than that of free boronic acids [2]. We recently incorporated pinacolboronate ester moiety into poly(ethylene glycol)-block-poly[(1,3-dioxane-5-ethyl) methyl acrylate] [7,8]. The resulting diblock copolymers poly(ethylene glycol)-block-poly[(2-phenylboronic esters-1,3-dioxane-5-ethyl) methylacrylate], abbreviated as PEG-b-PPBDEMA, formed nanostructures in aqueous solution and responded to glucose through transesterification reaction at $pH = 7.4$ where the glucose molecules took away the phenylboronate ester (PBE) moiety and detached it from the block copolymer (Fig. 1) [7,8]. The change in chemical structure of the hydrophobic core after reacting with glucose was monitored by 1H NMR [7]. Characteristic phenyl ring signals diminished due to removal of phenylborate ester moiety from the polymer architecture in the presence of glucose. The *in vitro* insulin release profiles revealed glucose-responsive behavior of the polymeric nanostructures at $pH 7.4$ and $37^\circ C$, which were affected by glucose concentration and chemical composition of the diblock polymers [7].

Precise control of the shapes of nanostructures in drug-delivery applications has been recognized as an important factor that affects the *in vivo* outcome [9]. For example, cylindrical micelles showed longer *in vivo* circulation times compared to analogous spherical morphologies [10]. Therefore, understanding the shape, size, and interaction of block copolymer assemblies is important to fully understand their performances, which will aid in better designing block copolymer assemblies for more efficient drug delivery. In aqueous solutions, morphological transitions between spherical micelles, cylindrical micelles, and vesicles or bilayers are observed by varying the hydrophobic-to-hydrophilic volume ratio of the block copolymers [11,12]. However, additional interactions such as hydrogen bonding, π - π interaction, and crystallization enrich the structures that block copolymers can form [13,14].

Dynamic light scattering (DLS), static light scattering, and transmission electron microscopy (TEM) have been frequently used to generate structural information of micelles and vesicles formed by PBA-containing block copolymers [4,5,7,8,15]. Small-angle neutron scattering (SANS) and small-angle X-ray scattering (SAXS) are powerful complementary techniques for revealing structures on the nano-meter scale and have been used to monitor *in situ* structural changes of block copolymer and surfactant assemblies [16–20]. In this work, self-assembled structures of PBE-containing diblock copolymers in water were studied using SANS for the first time. Vesicles were found in aqueous solutions, and their structural changes upon addition of glucose and sodium hydroxide were studied through SANS.

2. Experimental

2.1. Materials

Deuterium oxide and deuterated sodium hydroxide (40 wt.% in D_2O) were purchased from Cambridge Isotope Laboratories. Sodium dideuterium phosphate and disodium deuterium phosphate were purchased from C/D/N Isotopes, Inc. Tetrahydrofuran (THF) and glucose were purchased from Beijing Chemical Works. Detailed information of synthesis and characterization of the diblock copolymers can be found elsewhere [7,8]. The number averaged molecular weight of the diblock copolymer is measured to be 17,800 and the M_w/M_n is 1.46. The M_n measured by NMR is 25,500 g/mol. The degree of polymerization of PEG block is calculated to be 110 and that of the PPBDEMA block is estimated as 75.

2.2. Molecular weight measurement

The molecular weights and polydispersity index of the polymers were determined with Waters 515–2410 gel permeation chromatograph (GPC) instrument equipped with Styragel HT6E-HT5-HT3 chromatographic column following a guard column and a differential refractive-index detector. The measurements were performed using tetrahydrofuran (THF) as eluent (flow rate of 1.0 mL/min at $30^\circ C$) and a series of narrow polystyrene standards for the calibration.

2.3. Preparation of diblock copolymer nanostructures

5.0 mg polymer dissolved in 0.5 mL THF was added into 5 mL D₂O under vigorous stirring. The mixed solution was dialyzed against D₂O using dialysis membranes (MWCO 3500 Da), and D₂O was replenished every 6 h for 2 days. The solutions were stored at 4 °C before use. 20 μL 0.25 M deuterated phosphate-buffered saline (PBS) was introduced to 1 mL polymer solution prior to SANS experiment. The final solution concentration for all the samples was 0.1 wt.%. The critical micelle concentration (CMC) of the diblock copolymer in water was measured to be 6.5 mg L⁻¹ or 0.00065 wt.% by fluorescence probe technique using pyrene as the fluorescence dye.

2.4. SANS measurements

The measurements were performed at the Oak Ridge National Laboratory (ORNL) and National Institute of Standards and Technology (NIST). Preliminary experiment at ORNL was carried out on the Bio-SANS beamline. Two sample-to-detector distances (SDDs) (1.7 and 14.5 m) with a detector offset of 40 cm and a neutron wavelength of $\lambda = 6 \text{ \AA}$ were used to cover scattering vectors ($q = \frac{4\pi \sin \theta}{\lambda}$, 2θ is the scattering angle) ranging from 0.003 to 0.4 \AA^{-1} . The scattering intensity was put on an absolute scale by calibration with a standard sample. Final experiment at NIST was carried out on the NGB30 30 m beamline of the Cold Neutron Research Facility. Three SDDs (1.33, 4.0 and 13.17 m) with a detector offset of 25 cm at 1.33 m and a neutron wavelength of $\lambda = 6 \text{ \AA}$ were used to cover scattering vectors ranging from 0.003 to 0.4 \AA^{-1} . The scattering intensity was put on an absolute scale by calibration with direct beam flux. Samples for measurement at 37 °C were loaded into quartz cells with thickness of 2.0 mm. NCNR software package for SANS data analysis (https://www.ncnr.nist.gov/programs/sans/data/red_anal.html) was used in this study. Instrument resolution was included in the data analysis.

2.5. SANS data analysis

The absolute SANS intensity for monodisperse particles in solutions is given by [21]

$$I(q) = nP(q) \quad (1)$$

where n is the number density of the particles.

(1) Form factor of a core-shell spherical micelle is given as

$$P(q) = \left\{ \left(\frac{4\pi R_{core}^3}{3} \right) (\rho_{core} - \rho_{shell}) [3j_1(qR_{core}) / (qR_{core})] + \left(\frac{4\pi R_{micelle}^3}{3} \right) (\rho_{shell} - \rho_{solvent}) [3j_1(qR_{micelle}) / (qR_{micelle})] \right\}^2 \quad (2)$$

where R_{core} and $R_{micelle}$ are the radii of the micelle core and whole micelle, respectively; ρ_{core} , ρ_{shell} and $\rho_{solvent}$ are the scattering length density (SLD) of the core, corona, and solvent (assuming a homogeneous density distribution in each of the domains), respectively; $j_1(y)$ is the first-order spherical Bessel function.

Letting $\rho_{core} = \rho_{solvent}$, the scattering function from spherical vesicles with a uniform density in the bilayer is obtained.

(2) Form factor of a core-shell ellipsoidal micelle is given as

$$P(q) = \int_0^1 |F(q, r_i, \alpha)|^2 d\alpha \quad (3)$$

$$F(q, R_i, \alpha) = 3(\rho_{core} - \rho_{shell}) V_{core} j_1(u_{core}) / u_{core} + 3(\rho_{shell} - \rho_{solvent}) V_{shell} j_1(u_{shell}) / u_{shell} \quad (4)$$

where $V_{core} = \left(\frac{4\pi}{3}\right) R_{min,c} R_{maj,c}^2$, $V_{shell} = \left(\frac{4\pi}{3}\right) R_{min,s} R_{maj,s}^2$, $u_{core} = q \left[R_{maj,c}^2 (1 - \alpha^2) + R_{min,c}^2 \alpha^2 \right]^{\frac{1}{2}}$, $u_{shell} = q \left[R_{maj,s}^2 (1 - \alpha^2) + R_{min,s}^2 \alpha^2 \right]^{\frac{1}{2}}$, $R_{maj,c}$ and $R_{min,c}$ are the radii of the major and minor axes of core, $R_{maj,s}$ and $R_{min,s}$ are the radii of the major and minor axes of the micelle. The shell thickness along the major axis is given by the difference between $R_{maj,s}$ and $R_{maj,c}$; the shell thickness along the minor axis is given by the difference between $R_{min,s}$ and $R_{min,c}$.

(3) The form factor of an ellipsoid with R_a and R_b is given as

$$P(q) = (\rho_{ell} - \rho_{solvent})^2 \int_0^1 F^2 \left[qR_b (1 + x^2 (v^2 - 1))^{1/2} \right] dx \quad (5)$$

where $F(z) = 3V_{ell} \frac{\sin z - z \cos z}{z^3}$, $V_{ell} = \frac{4\pi}{3} R_a R_b^2$, $v = \frac{R_a}{R_b}$ and v is the elliptical eccentricity.

Assuming a Schulz distribution of the particle sizes: [22]

$$f(r) = \frac{r^z}{\Gamma(z+1)} \left(\frac{z+1}{\langle r \rangle} \right)^{z+1} \exp \left[\frac{-r(z+1)}{\langle r \rangle} \right] \quad (6)$$

The polydispersity σ is given as $\sigma^2 = 1/(z+1)$.

The averaged form factor is then given as

$$\overline{P(q)} = \int P(q)V_p^2 f(r)dr / \int V_p^2 f(r)dr$$

The neutron scattering length density (SLD) of D₂O is $6.34 \times 10^{-6} \text{ \AA}^{-2}$, of PEG is $0.67 \times 10^{-6} \text{ \AA}^{-2}$ using a mass density of 1.196 g mL^{-1} [23]. The mass density of PPBDEMA was not found; SciFinder^R gives a predicted mass density of the monomer, 1.08 g mL^{-1} . A SLD of $1.34 \times 10^{-6} \text{ \AA}^{-2}$ was obtained using that number. The scattering in the buffer solution produced a flat background in the higher q region; however, background subtraction was a challenge because of the low polymer concentration. It was found that the scattering intensity of the background was comparable to that of the D₂O buffer for some samples and background subtraction resulted negative values of scattering intensity. Therefore the background subtraction was not performed. This does not affect the data fitting itself since a constant background over the measured q range was used during that process, as shown before [24].

2.6. DLS analysis

The particle size of nanostructures was measured with “Zetaplus” zeta potential analyzer (Brookhaven Instrument) equipped with ZetaPlus Particle Sizing software and with 35 mW solid state laser operated at a laser light wavelength of 660 nm. The size measurements were carried out at 37 °C at a scattering angle of 90°.

3. Results and discussion

In this work, we were interested in size and shape of the nanostructures assembled through PEG-b-PPBDEMA under different conditions. Dilute polymer solutions were used to minimize inter-particle interactions. The DLS data of 0.1 wt.% polymer in 0.005 M PBS buffer was shown in Fig. 2 and it yielded an average hydrodynamic radius of 34 nm with a polydispersity of 0.13. Fig. 3a presents SANS data of 0.1 wt.% polymer in 0.005 M PBS buffer. Prior to addition of glucose, the scattering curve is best described by a polydisperse spherical vesicular model with a uniform shell, which is equivalent to a spherical core-shell model with the core filled with water. A homogenous density distribution in both the core and shell was assumed. This simplified model described the SANS data rather well with a reduced χ^2 of 3.5. The scattering in the local structures of vesicles (around 0.1 \AA^{-1}) [16,25], such as the conformation of the PEG chains, was difficult to extract due to very low polymer concentration. This, in turn, prohibited applying more sophisticated models to analyze the data. Since the quality of the fit was good, a core-shell model with three layers in the shell [16] was not adopted. More sophisticated models will not lead to a unique set of parameters. SANS analysis generated a radius of 33 nm and a polydispersity of 0.25. The SLD of the shell obtained from the fit was $2.1 \times 10^{-6} \text{ \AA}^{-2}$, that is higher than both the SLDs of PEG and PPBDEMA blocks, suggesting that the shell is swollen with D₂O. Using the volume-averaged SLD over the two blocks, the volume fraction of water in the vesicle was estimated to be about 18%. Inclusion of PEG block in the shell would lead to larger volume fraction of water in the shell. The water content in the hydrophobic membrane of block copolymer vesicles can reach as high as 60–70% while still maintains their integrity [25]. Vesicles are interesting delivery systems for drugs encapsulated either in their aqueous interior or in their hydrophobic bilayer [6,25,26]. It has been suggested that spherical micelles are expected for block polymers with hydrophilic mass fraction greater than 45%, whereas block copolymers with lower hydrophilic mass fraction typically self-assemble into vesicles [27]. Considering the weight percentage of PEG in the diblock copolymer, 24, formation of vesicles in water is consistent with this rule.

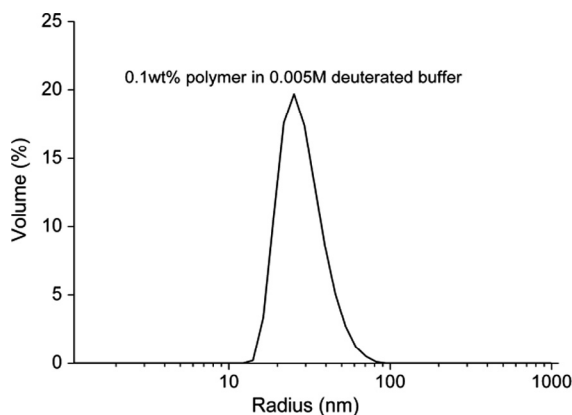


Fig. 2. Hydrodynamic radius distribution of PEG-b-PPBDEMA vesicles.

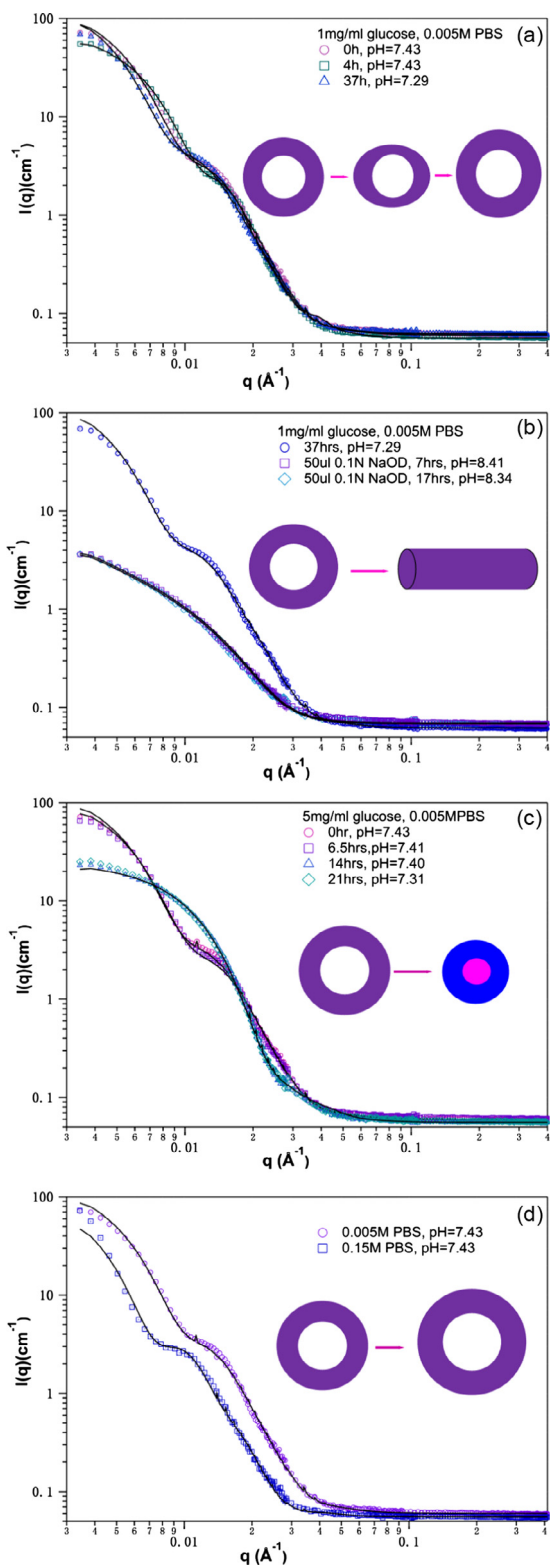


Fig. 3. (a) SANS data of 0.1 wt.% polymer in 0.1 wt.% glucose solution as a function of time. (b) Addition of 0.1N NaOD to the polymer solution 37 h after glucose addition. (c) SANS data of 0.1 wt.% polymer in 0.5 wt.% glucose solution as a function of time. (d) SANS data of the polymer in PBS buffer solutions with different molar concentration. Solid lines are fits to model functions. The SANS data in figure a and c were shifted vertically for the sake of clarity and included in the [supplementary materials](#).

Table 1
Structural parameters extracted from model fits of the vesicles.

Time after glucose addition (0.1%, 0.005 M PBS) (h)	R_{core} or $R_{\text{major_core}}$ (Å)	$R_{\text{minor_core}}$ (Å)	t_{shell} or $t_{\text{major_shell}}$ (Å)	$t_{\text{minor_shell}}$ (Å)	SLD of the shell (\AA^{-2})	Volume of a vesicle (\AA^3)
0	191		142		$2.1\text{E}-6$	$1.55\text{E}+08$
4	177	148	238	54	$1.7\text{E}-6$	$1.46\text{E}+08$
15	181		147		$1.8\text{E}-6$	$1.48\text{E}+08$
26	193		147		$1.8\text{E}-6$	$1.65\text{E}+08$
37	227		140		$2.2\text{E}-6$	$2.07\text{E}+08$
Vesicles in 0.15 M PBS	309		182		$2.1\text{E}-6$	$4.96\text{E}+08$

Errors associated with sizes obtained from the modeling are usually less than 1.5 Å.

As shown in Table 1, the obtained inner radius (radius of lumen), R_{core} , is 191 Å, and the thickness of the shell, t_{shell} , is 142 Å. The thickness of the shell was then compared with the sizes of the two blocks. A contour length of a fully stretched PEG chain with a DP of 110 was estimated to be 400 Å; a root-mean-square end-to-end distance of an ideal chain was estimated to be 66 Å [28]. The molecular parameters, i.e., Kuhn length, etc., of the PPBDEMA block are unknown; hence, a common homopolymer that is similar to the main chain of the PPBDEMA, poly(methyl methacrylate) (PMMA), was used. The contour length of a fully stretched PMMA chain with a DP of 75 was estimated to be 194 Å; the root-mean-square end-to-end distance of an ideal chain was estimated to be 57 Å [28]. Assuming no interdigitation, the thickness of the bilayer formed by the diblock copolymers was roughly estimated as $2 \times (66 + 57) = 246$ Å. Introduction of PBE groups will increase the end-to-end distance because of steric hindrance effect. The shell thickness extracted from SANS data corresponds to about a half of the bilayer thickness, suggesting an interdigitated bilayer of the vesicles [29]. Another possibility is that the diffuse interface between PEG chains and water was not considered in the core-shell model used here.

Glucose was then introduced into the polymer solution to reach a concentration of 0.1 wt.% and variation of the structure of the vesicles as a function of time was monitored by SANS. The scattering curve from the polymer solution could not be fitted with the spherical core-shell model 4 h after the addition of glucose. An oblate ellipsoidal core-shell model fit the data well, with a polydispersity of 0.25 and a reduced χ^2 of 3.0. A homogenous density distribution in both the core and shell was assumed. The sizes from the fits are as follows: major inner radius, $R_{\text{major_core}} = 177$ Å; minor inner radius, $R_{\text{minor_core}} = 148$ Å; major shell thickness, $t_{\text{major_shell}} = 238$ Å; and minor shell thickness, $t_{\text{minor_shell}} = 54$ Å. We find that the volume of the whole vesicle dropped after addition of glucose. One would expect the vesicles to swell with improved overall hydrophilicity of the diblock copolymers as a result of the reaction between glucose and PBE moiety (Fig. 1). This decrease in volume was thus proposed to be caused by osmotic pressure generated by glucose. The volume of the aqueous interior decreased in response to the increased osmotic pressure. Meanwhile, the SLD of the shell also decreased to $1.7 \times 10^{-6} \text{\AA}^{-2}$ due to dehydration by glucose. The lumen of the vesicles deformed significantly, giving an aspect ratio of 4.4.

With more glucose molecules reacting with the PBE segments and diffusing into the aqueous interior, the vesicles were expected to become larger, which was indeed the case at longer times. As shown in Table 1, the volume of the vesicles increased 15 h later. SANS curves at 15, 26, and 37 h were again fitted well with the spherical vesicular model, with a reduced χ^2 varying from 2.7 to 3.0, and a polydispersity from 0.26 to 0.28. The SLD of the shell increased from $1.7 \times 10^{-6} \text{\AA}^{-2}$ to $2.2 \times 10^{-6} \text{\AA}^{-2}$ due to increased hydration. The shell thickness was found roughly constant while the volume of the aqueous interior increased. This suggests that an average distance between polymer chains in the shell increased due to enhanced hydrophilicity. It is in accordance with a prior study which proposed that increased hydrophobicity of polymers in the shell of vesicles led to greater attractive forces between the polymers [25]. It was noticed that the pH of the polymer solution decreased to 7.29 after 37 h. The decrease in pH was caused by the ionization of phenylboronate–glucose complex that consumed hydroxide ions in the buffer solutions. This change in pH also slowed down the reaction between glucose and the PBE moieties in the diblock copolymers.

In addition to glucose, increasing the pH of the polymer solution also increases the hydrophilicity of the PBE-containing block via increased ionization. The stability of PBE is known to be pH dependent and it increases with increasing pH within a certain range [30]. In a recent study, a brushlike block copolymer containing the PPBDEMA block was synthesized and its pH and glucose-responsive properties were tested [31]. The block copolymers associated into micelles in water and they were found to dissociate upon elevating pH to 8.8. This was attributed to increased ionization of the PBDEMA block [31]. With further increasing pH to 12, saponification took place [31]. In this work, NaOD solution was added to the vesicular solution 37 h after the addition of glucose. SANS data were collected 17 h after introducing NaOD, and the resulting pH of the polymer solution was 8.34. Based on the previous study [31], it was believed that ionization took place for the PBDEMA block at this pH. As shown in Fig. 3b, the SANS curve changed significantly both in intensity and shape. Although the transesterification reaction shown in Fig. 1 might continue under alkaline conditions, this drastic change in the SANS pattern was apparently caused by elevation of the pH. The scattering intensity at $q = 0.0034 \text{\AA}^{-1}$, the lowest q value in this work, decreased from approximately 80 to 4 cm^{-1} , suggesting that a significant fraction of the vesicles had dissociated in alkaline solution. The scattering data in the low- q region followed power-law decay with an exponent of -1 , indicating presence of cylindrical particles. Because of lower scattering intensity, the scattering from unassociated diblock copolymers (unimers) cannot be ignored. In principle, the scattering data can be analyzed using a linear combination of scattering from cylinders and unimers

[20]. However, a set of parameters could not be uniquely determined in part because a fully dissociated region was not achieved, and the radius of gyration of the unimers could not be obtained.

The glucose concentration of 0.1 wt.% corresponds to that of the normal level in blood. To test the effect of higher glucose concentration on the structure of the vesicles, a vesicular solution with a glucose concentration of 0.5 wt.% was studied through SANS (Fig. 3c). Six and an half hours after glucose was added, vesicles kept their spherical shape with $R_{in} = 174 \text{ \AA}$, $t_{shell} = 140 \text{ \AA}$; however, the volume of individual vesicles decreased. This phenomenon is similar to the structural change induced by 0.1 wt.% glucose at longer times. A dramatic change in the SANS pattern was observed 14 h after glucose was added, which did not occur for the polymer solution with glucose concentration of 0.1%. The scattering intensity at low- q decreased from $80 \text{ to } 20 \text{ cm}^{-1}$, suggesting the dissociation of vesicles. The SANS curve was fitted with uniform oblate ellipsoids with a reduced χ^2 of 3.9. A fit to the ellipsoidal model gives the following sizes: the radius of the axis of rotation is 114 \AA and that of the major axis is 245 \AA . Scattering from the polymers in the shell [32] was not detected in the high- q region for the same reason as described above. Therefore, only an overall size and shape of the micelles were obtained.

A transition from vesicles to cylindrical micelles and finally spherical micelles took place with increasing hydrophilic volume of the block copolymers [33,34]. The observed morphological changes induced by the elevation of pH or addition of higher concentration of glucose are consistent with this rule. Most importantly, the results show a morphological transition for the vesicles in the presence of glucose, which is an aspect that has a significant influence on the design of drug carriers and interpretation of drug release profiles.

Fig. 3d compares the effect of molar concentration of PBS buffer on the stability of the vesicles. Six hours after mixing the polymer with 0.005 M PBS buffer, scattering intensity decreased, suggesting that a fraction of the vesicles had dissociated. The breakup of the vesicles was caused by an increased ionization of the PBE-containing blocks. As shown in a previous study, higher ionic strength leads to decreased pK_a values [35]. Therefore, PBE-containing blocks have a lower pK_a in 0.15 M PBS buffer than that in the 0.005 M PBS buffer, resulting in increased ionization. During a preliminary test, the stability of diblock copolymers assemblies in PBS buffer with lower molarity was checked by SANS and the data were shown in supplementary materials. SANS data suggested that vesicles in 0.01 M PBS buffer were stable up to 3 days.

The SANS curve of the polymer in 0.15 M PBS buffer was consistent with a spherical vesicular model where the volume of individual vesicles increased in comparison to that from 0.005 M PBS buffer. This increase in size was caused by the increased hydrophilicity of the diblock copolymer because of ionization and repulsion between ionized PBE segments in the shell of the vesicles. This finding is similar to that of a prior work, which reported volume expansion of vesicles because of the increased ionization of one of the shell-forming blocks [36].

4. Conclusions

PEG-*b*-PBDEMA with a PEG content of 24 wt.% formed vesicles with an interdigitated bilayer that presented interesting morphological responses to glucose, as revealed by SANS. Vesicles contracted and deformed initially after glucose addition because of the presence of the aqueous interior. Continuing reactions between glucose and the PBDEMA blocks led to increased hydrophilic-to-hydrophobic volume ratio that eventually induced both dissociation and shape transformation. Increasing pH of the vesicular solution resulted in increased degree of ionization of the PBDEMA blocks, thereby also increasing the hydrophilic to hydrophobic volume ratio. Higher glucose concentration led to faster reaction rate that led to drastic shape changes of vesicles while the vesicles in the solution of lower glucose concentration were relatively stable. The vesicles expanded in volume and dissociated in the PBS buffer with a molarity of 0.15 M. The results provide a new comparative insight into the solution structure of PBE-containing block copolymers and form the basis for future work on the mechanism of insulin encapsulation and release under physiological conditions.

Acknowledgements

Gang Cheng's travel to neutron facilities was supported in part by the joint funds of National Natural Science Foundation of China and Large Scale Scientific Facility of Chinese Academy of Science (U1432109). Jin Yang acknowledges National Natural Science Foundation of China (21374005). Gang Cheng thanks Drs. Daisuke Sawada and Sai Venkatesh Pingali of ORNL for the help with SANS experiments. This work utilized facilities supported in part by the US National Science Foundation under Agreement No. DMR-1508249. We acknowledge the support of the National Institute of Standards and Technology, U.S. Department of Commerce, in providing the neutron research facilities used in this work. The identification of commercial products does not imply endorsement by the National Institute of Standards and Technology (NIST) nor does it imply that these are the best for the purpose. The research at Oak Ridge National Laboratory's High Flux Isotope Reactor was sponsored by the Scientific User Facilities Division, Office of Basic Energy Sciences, and U.S. Department of Energy.

Appendix A. Supplementary material

Supplementary data associated with this article can be found, in the online version, at <http://dx.doi.org/10.1016/j.eurpolymj.2016.08.019>.

References

- [1] R. Ma, L. Shi, Phenylboronic acid-based glucose-responsive polymeric nanoparticles: synthesis and applications in drug delivery, *Polym. Chem.* 5 (5) (2014) 1503–1518.
- [2] W.L.A. Brooks, B.S. Sumerlin, Synthesis and applications of boronic acid-containing polymers: from materials to medicine, *Chem. Rev.* 116 (3) (2016) 1375–1397.
- [3] D. Roy, J.N. Cambre, B.S. Sumerlin, Triply-responsive boronic acidblock copolymers: solution self-assembly induced by changes in temperature, pH, or sugar concentration, *Chem. Commun.* 16 (2009) 2106–2108.
- [4] J. Zou, S. Zhang, R. Shrestha, K. Seetho, C.L. Donley, K.L. Wooley, PH-Triggered reversible morphological inversion of orthogonally-addressable poly(3-acrylamidophenylboronic acid)-block-poly(acrylamidoethylamine) micelles and their shell crosslinked nanoparticles, *Polym. Chem.* 3 (11) (2012) 3146–3156.
- [5] Q. Guo, Z. Wu, X. Zhang, L. Sun, C. Li, Phenylboronate-diol crosslinked glycopolymeric nanocarriers for insulin delivery at physiological pH, *Soft Matter* 10 (6) (2014) 911–920.
- [6] H. Kim, Y.J. Kang, S. Kang, K.T. Kim, Monosaccharide-responsive release of insulin from polymersomes of polyboroxole block copolymers at neutral pH, *J. Am. Chem. Soc.* 134 (9) (2012) 4030–4033.
- [7] Y. Yao, L. Zhao, J. Yang, J. Yang, Glucose-responsive vehicles containing phenylborate ester for controlled insulin release at neutral pH, *Biomacromolecules* 13 (6) (2012) 1837–1844.
- [8] Y. Yao, X. Wang, T. Tan, J. Yang, A facile strategy for polymers to achieve glucose-responsive behavior at neutral pH, *Soft Matter* 7 (18) (2011) 7948–7951.
- [9] S. Venkataraman, J.L. Hedrick, Z.Y. Ong, C. Yang, P.L.R. Ee, P.T. Hammond, et al, The effects of polymeric nanostructure shape on drug delivery, *Adv. Drug. Deliv. Rev.* 63 (14–15) (2011) 1228–1246.
- [10] N. Petzetakis, A.P. Dove, R.K. O'Reilly, Cylindrical micelles from the living crystallization-driven self-assembly of poly(lactide)-containing block copolymers, *Chem. Sci.* 2 (5) (2011) 955–960.
- [11] Y.-Y. Won, A.K. Brannan, H.T. Davis, F.S. Bates, Cryogenic transmission electron microscopy (Cryo-TEM) of micelles and vesicles formed in water by poly(ethylene oxide)-based block copolymers, *J. Phys. Chem. B* 106 (13) (2002) 3354–3364.
- [12] M.J. Greenall, P. Schuetz, S. Furlzeland, D. Atkins, D.M.A. Buzza, M.F. Butler, et al, Controlling the self-assembly of binary copolymer mixtures in solution through molecular architecture, *Macromolecules* 44 (13) (2011) 5510–5519.
- [13] J.R. McDaniel, I. Weitzhandler, S. Prevost, K.B. Vargo, M.-S. Appavou, D.A. Hammer, et al, Noncanonical self-assembly of highly asymmetric genetically encoded polypeptide amphiphiles into cylindrical micelles, *Nano Lett.* 14 (11) (2014) 6590–6598.
- [14] L. Yin, T.P. Lodge, M.A. Hillmyer, A stepwise, “Micellization–Crystallization” route to oblate ellipsoidal, cylindrical, and bilayer micelles with polyethylene cores in water, *Macromolecules* 45 (23) (2012) 9460–9467.
- [15] W. Scarano, H.T.T. Duong, H. Lu, P.L. De Souza, M.H. Stenzel, Folate conjugation to polymeric micelles via boronic acid ester to deliver platinum drugs to ovarian cancer cell lines, *Biomacromolecules* 14 (4) (2013) 962–975.
- [16] J. Habel, A. Ogonna, N. Larsen, S. Cherre, S. Kynde, S.R. Midtgaard, et al, Selecting analytical tools for characterization of polymersomes in aqueous solution, *RSC Adv.* 5 (97) (2015) 79924–79946.
- [17] R. Lund, L. Willner, D. Richter, P. Lindner, T. Narayanan, Kinetic pathway of the cylinder-to-sphere transition in block copolymer micelles observed in situ by time-resolved neutron and synchrotron scattering, *ACS Macro Lett.* 2 (12) (2013) 1082–1087.
- [18] G.V. Jensen, R. Lund, J. Gummel, T. Narayanan, J.S. Pedersen, Monitoring the transition from spherical to polymer-like surfactant micelles using small-angle X-Ray scattering, *Angew. Chem. Int. Ed.* 53 (43) (2014) 11524–11528.
- [19] R. Lund, V. Pipich, L. Willner, A. Radulescu, J. Colmenero, D. Richter, Structural and thermodynamic aspects of the cylinder-to-sphere transition in amphiphilic diblock copolymer micelles, *Soft Matter* 7 (4) (2011) 1491–1500.
- [20] K.E.B. Doncom, A. Pitto-Barry, H. Willcock, A. Lu, B.E. McKenzie, N. Kirby, et al, Complementary light scattering and synchrotron small-angle X-ray scattering studies of the micelle-to-unimer transition of polysulfobetaines, *Soft Matter* 11 (18) (2015) 3666–3676.
- [21] J.S. Pedersen, Analysis of small-angle scattering data from colloids and polymer solutions: modeling and least-squares fitting, *Adv. Colloid Interface Sci.* 70 (1997) 171–210.
- [22] G. Cheng, Y.B. Melnichenko, G.D. Wignall, F. Hua, K. Hong, J.W. Mays, Small angle neutron scattering study of conformation of oligo(ethylene glycol)-grafted polystyrene in dilute solutions: effect of the backbone length, *Macromolecules* 41 (24) (2008) 9831–9836.
- [23] T. Zinn, L. Willner, R. Lund, V. Pipich, M.-S. Appavou, D. Richter, Surfactant or block copolymer micelles? Structural properties of a series of well-defined n-alkyl-PEO micelles in water studied by SANS, *Soft Matter* 10 (28) (2014) 5212–5220.
- [24] G. Cheng, M.S. Kent, L. He, P. Varanasi, D. Dibble, R. Arora, et al, Effect of ionic liquid treatment on the structures of lignins in solutions: molecular subunits released from lignin, *Langmuir* 28 (32) (2012) 11850–11857.
- [25] N.J. Warren, O.O. Mykhaylyk, A.J. Ryan, M. Williams, T. Doussineau, P. Dugourd, et al, Testing the vesicular morphology to destruction: birth and death of diblock copolymer vesicles prepared via polymerization-induced self-assembly, *J. Am. Chem. Soc.* 137 (5) (2015) 1929–1937.
- [26] C. Gonzato, M. Semsarilar, E.R. Jones, F. Li, G.J.P. Krooshof, P. Wyman, et al, Rational synthesis of low-polydispersity block copolymer vesicles in concentrated solution via polymerization-induced self-assembly, *J. Am. Chem. Soc.* 136 (31) (2014) 11100–11106.
- [27] D.E. Discher, A. Eisenberg, Polymer vesicles, *Science* 297 (5583) (2002) 967–973.
- [28] M. Rubinstein, R.H. Colby, *Polymer Physics*, OUP Oxford, 2003.
- [29] A. Blanz, S.P. Armes, A.J. Ryan, Self-assembled block copolymer aggregates: from micelles to vesicles and their biological applications, *Macromol. Rapid Commun.* 30 (4–5) (2009) 267–277.
- [30] C. Yu, V.W.-W. Yam, Glucose sensing via polyanion formation and induced pyrene excimer emission, *Chem. Commun.* 11 (2009) 1347–1349.
- [31] W. Yuan, L. Li, H. Zou, Thermo- and glucose-responsive micelles self-assembled from phenylborate ester-containing brush block copolymer for controlled release of insulin at physiological pH, *RSC Adv.* 5 (98) (2015) 80264–80268.
- [32] J.S. Pedersen, M.C. Gerstenberg, Scattering form factor of block copolymer micelles, *Macromolecules* 29 (4) (1996) 1363–1365.
- [33] C. Zhou, M.A. Hillmyer, T.P. Lodge, Micellization and micellar aggregation of poly(ethylene-alt-propylene)-b-poly(ethylene oxide)-b-poly(N-isopropylacrylamide) triblock terpolymers in water, *Macromolecules* 44 (6) (2011) 1635–1641.
- [34] Q. Jin, C. Luy, J. Ji, S. Agarwal, Design and proof of reversible micelle-to-vesicle multistimuli-responsive morphological regulations, *J. Polym. Sci., Part A: Polym. Chem.* 50 (3) (2012) 451–457.
- [35] Y. Tian, T.A. Hatton, K.C. Tam, Dissociation and thermal characteristics of poly(acrylic acid) modified pluronic block copolymers in aqueous solution, *Polymer* 55 (16) (2014) 3886–3893.
- [36] H. Liu, Z. Guo, S. He, H. Yin, C. Fei, Y. Feng, CO₂-driven vesicle to micelle regulation of amphiphilic copolymer: random versus block strategy, *Polym. Chem.* 5 (16) (2014) 4756–4763.